Journal of Pharmaceutical and Biomedical Analysis 185 (2020) 113249

Contents lists available at ScienceDirect

Journal of Pharmaceutical and Biomedical Analysis

journal homepage: www.elsevier.com/locate/jpba

Metal-polymer hybrid nanomaterial for impedimetric detection of human papillomavirus in cervical specimens

Karen Y.P.S. Avelino[a,b], Léony S. Oliveira[b], Norma Lucena-Silva[c,d], Celso Pinto de Melo[e], César A.S. Andrade[a,b], Maria D.L. Oliveira[a,b,*]

[a] Programa de Pós-Graduação em Inovação Terapêutica, Universidade Federal de Pernambuco, 50670-901 Recife, PE, Brazil
[b] Laboratório de Biodispositivos Nanoestruturados, Departamento de Bioquímica, Universidade Federal de Pernambuco, 50670-901 Recife, PE, Brazil
[c] Instituto Aggeu Magalhães, Fundação Oswaldo Cruz (Fiocruz), 50670-420 Recife, PE, Brazil
[d] Laboratório de Biologia Molecular, Departamento de Oncologia Pediátrica, Instituto de Medicina Integral Professor Fernando Figueira (IMIP), 50070-550 Recife, PE, Brazil
[e] Departamento de Física, Universidade Federal de Pernambuco, 50670-901 Recife, PE, Brazil

ARTICLE INFO

Article history:
Received 9 October 2019
Received in revised form 28 February 2020
Accepted 8 March 2020
Available online 9 March 2020

Keywords:
Biosensor
Polyaniline
Gold nanoparticle
Human papillomavirus
Electrochemical impedance spectroscopy

ABSTRACT

The human papillomavirus (HPV) is one of the main sexually transmitted pathogens that infect the anogenital epithelium and mucous membranes. HPV genotypes can be classified as high and low oncogenic risk, with infection by the former resulting in cervical cancer in approximately 100 % of the cases. In this work, we developed an ultrasensitive electrochemical biosensor for the detection and identification of different HPV genotypes. A nanostructured platform based on a matrix of polyaniline (PANI) containing gold nanoparticles (AuNps) was designed for the chemical immobilization of a DNA probe capable of recognizing different HPV types. Cyclic voltammetry (CV), electrochemical impedance spectroscopy (EIS), and atomic force microscopy (AFM) were used to characterize the genosensor. The impedimetric responses indicate that the proposed sensor was able to detect HPV (types 6, 11, 16, 31, 33, 45, and 58) in cervical specimens (cDNA samples). We obtained different profiles of electrochemical responses for the high and low-risk HPV genotypes. By adopting a three-dimensional quantitative analysis of impedance response variables, it was possible to identify the existence of a pattern of association for samples of high oncogenic risk, which may lead to the differential diagnosis of HPV. The biosensor demonstrated an excellent analytical performance for the detection of HPV genotypes with high sensibility and selectivity. The genosensor exhibited a linear range of response in the 1 pg μL^{-1} to 100 pg μL^{-1} range. Besides, a limit of detection (LOD) of 2.74 pg μL^{-1} and 7.43 pg μL^{-1} was obtained for HPV11 and HPV16, respectively, with regression coefficients of 99.88 % and 99.47 %. Thus, the proposed sensor may serve as a good prognostic indicator for patients infected with papillomavirus.

1. Introduction

HPV is a non-enveloped double-stranded DNA virus responsible for infections in the mucous membranes and anogenital epithelium. This pathogen, which presents high incidence and prevalence among youths and adults, is the most common sexually transmitted virus [1]. Currently, more than 200 HPV genotypes are known and subdivided according to their oncogenic potential. While low-risk HPV types (6, 11, 40, 42, 43, 44, 53, 54, 61, 72, 73, and 81) are associated with the appearance of genital warts, high-risk HPV types (16, 18, 31, 33, 35, 39, 45, 51, 52, 56, 58, 59, and 68) are responsible for cytogenetic changes associated to the development of cancers such as cervical, penile, vaginal, vulvar, and anal cancer. Epidemiological studies have demonstrated that approximately 93–100 % of the cases of invasive cervical cancer are correlated to HPV type 16 and 18 [2].

The identification of the HPV type in clinical samples could provide for better patient prognosis and the subsequent implementation of therapeutic strategies to obtain satisfactory results. The molecular methods used for HPV screening can be classified into nucleic acid-hybridization assays (southern blotting, *in situ* hybridization and dot-blot hybridization), signal amplification assays (Hybrid Capture® 2 and Cervista® HPV) and nucleic-acid amplification assays (quantitative real-time polymerase chain reaction (RT-qPCR), PapilloCheck® and Cobas® 4800) [3]. Although

* Corresponding author at: Departamento de Bioquímica, UFPE, 50670-901, Recife, PE, Brazil.
E-mail address: m_danielly@yahoo.com.br (M.D.L. Oliveira).

https://doi.org/10.1016/j.jpba.2020.113249
0731-7085/

these tools are high-quality, they present limitations for extensive use in hospitals and laboratories, such as high acquisition costs for equipment, large amounts of purified DNA, limited sensitivity, and complex experimental protocols with extended analysis time [4]. The development of molecular assays for HPV detection with high accuracy and bioanalytical performance is of great relevance for the promotion of the health of infected patients.

Researchers in nanoscience and biotechnology have made significant progress in the development of new electronic devices such as biosensors. The functional strategy of these devices is based on the specificity of biological molecules and the analytical capacity of signal transduction methods. Also, electrochemical genosensors are based on the immobilization of nucleic acid segments on electrochemical transducers, with the response being related to the hybridization between a single-stranded DNA fragment and its complementary strand [5]. The electrochemical genosensors are potentially useful for clinical diagnosis due to their advantageous characteristics, such as low cost, sensitive detection, the possibility of real-time analysis and small sample requirement, requiring simple instrumentation that allows for miniaturization, portability, and automation [6].

Nanostructured platforms are effective interfaces between biomolecules and electrode surfaces that provide stable anchoring for recognition molecules without loss of biological activity. Numerous materials can be used to obtain nanostructured platforms, such as nanoparticles, nanotubes, nanowires, nanorods, nanopores, and quantum dots. Hybrid nanocomposites composed of the nanoparticles and conjugated polymers have become increasingly prominent in the field of electrochemical genosensors [7]. Gold nanoparticles and polyaniline (AuNp/PANI) hybrid composites have shown unique characteristics for the development of high-performance sensing platforms [8].

AuNps are a nanomaterial extensively used for the construction of biological sensors. AuNps are a well-know nanomaterial due to quantum size effect, shape-related optoelectronic characteristics, single-electron transition, surface plasmon band, fluorescence, magnetism, electric conductivity, and electrochemical characteristics [9]. Previous studies have shown that these metallic nanoparticles are essential components for interfacing biological recognition. Besides, AuNps exhibit high surface energy, enable the direct and effective transfer of electrons between the electrode and the biomolecule, and have a high relation between surface area and volume that provides a larger electrochemical area [10].

Of note, several approaches have been described for the incorporation of AuNps into polymer matrices to obtain hybrid nanocomposites with synergistic properties [11]. In this context, we highlight PANI, a polymer whose conductivity is sensitive to its oxidation state and pH of the microenvironment. The conductive form of PANI is the protonated polyemeraldine or polyemeraldine salt, whose conductivity is around 15 S cm^{-1}. PANI is an exciting material for use in biosensor interfaces since it can act as an effective mediator for electron transfer in redox or enzymatic reactions that contribute to the amplification of the analytical signal, leading to an increased sensitivity of the detection devices. Also, PANI can also be used as immobilization support for biological molecules that allow the preservation of their conformational properties [12].

In recent years, several innovative improvements have been made in DNA biosensors for the detection of papillomavirus and single nucleotide polymorphism. Electrochemical signal conversion methods are among the main types of transducers used in HPV biosensors [4]. Electrochemical markers, such as methylene blue, ferrocene, horseradish peroxidase, anthraquinone, and 1,10-phenanthroline ruthenium dichloride, have been used to evidence target recognition. Of note, nanomaterials associated with sensor devices enable a label-free ultrasensitive detection of HPV. Although significant advances have been obtained in electrochemical biosensors for HPV, most analyzes are performed with synthetic modeled DNA sequences (recombinant plasmids) due to the complexity of the human samples [3].

In this work, we developed a nanoelectrode based on AuNp/PANI hybrid composite for the sensitive diagnosis of HPV in cervical specimens. A degenerate DNA probe was attached on an AuNp/PANI-modified gold electrode through chemical interactions. We used atomic force microscopy (AFM) to examine the topographic characteristics of the nanostructured platform. We performed the ultrasensitive detection of different HPV genotypes (6, 11, 16, 31, 33, 45, and 58) in patients' clinical samples through cyclic voltammetry (CV) and electrochemical impedance spectroscopy (EIS). To the best of our knowledge, this study provides the first label-free sensor based on degenerate oligonucleotide sequence able to verify differences in electrochemical responses to HPV groups of high and low risk. Thus, the proposed DNA biosensor can be considered a promising system for the differential diagnosis of HPV with oncogenic prediction.

2. Materials and methods

2.1. Materials

Tetrachloroauric acid ($HAuCl_4$) and 3-mercaptopropyltrimethoxysilane (MPTMS - $HS(CH_2)_3Si(OCH_3)_3$) were purchased from Sigma Chemical (St. Louis, MO, USA). Aniline, potassium ferricyanide ($K_3[Fe(CN)_6]$), potassium ferrocyanide ($K_4[Fe(CN)_6]$), glutaraldehyde, sodium phosphate and alumina (α-Al_2O_3) were obtained from VETEC (SP, Brazil). Aniline was previously distilled under reduced pressure before use. All other reagents were of analytical grade and used as received. Deionized water was obtained using a Millipore system (Milli-Qplus, Billerica, USA).

2.2. Biological samples

The cervical samples were collected after the consent of the women patients. The study was previously approved by a research ethics committee (process n° CAAE 23698513.0.0000.5190). HPV genotypes recognition was based on the use of an MY11 probe with sequence (5′ to 3′) amine-GCM CAG GGW CAT AAY AAT GG, purchased from Invitrogen (USA). The recognition site of this degenerate primer is a conserved region of the HPV L1 gene. mRNA segments were extracted from cervical cells using Trizol and converted by reverse transcriptase to complementary DNA (cDNA). Positive (with genotype discrimination) or negative samples were previously characterized through real-time polymerase chain reaction (RT-PCR).

2.3. Preparation of the AuNp/PANI hybrid nanocomposite

Initially, aniline (0.03 mol L^{-1}), MPTMS (6.46×10^{-2} mol L^{-1}), and $HAuCl_4$ (0.81 mmol L^{-1}) were added to a round bottom flask containing ethanol under magnetic stirring (1100 rpm) for 48 h for obtaining AuNp/PANI hybrid nanocomposites. Subsequently, the AuNp/PANI hybrid nanocomposites were subjected to a centrifugation process at 12 000 rpm for 10 min for the segregation of large agglomerates. After, 500 μL of HCl (0.1 M) was added to AuNp/PANI solution to obtain positive electrical charges on PANI (via protonation reaction) and hydrolysis of the excess MPTMS [13].

2.4. Immobilization of the DNA probe in the AuNp/PANI hybrid nanocomposite

The bare gold electrode (φ =2 mm) was carefully polished with abrasive paper and Al_2O_3 paste (0.05 μm) and then rigorously

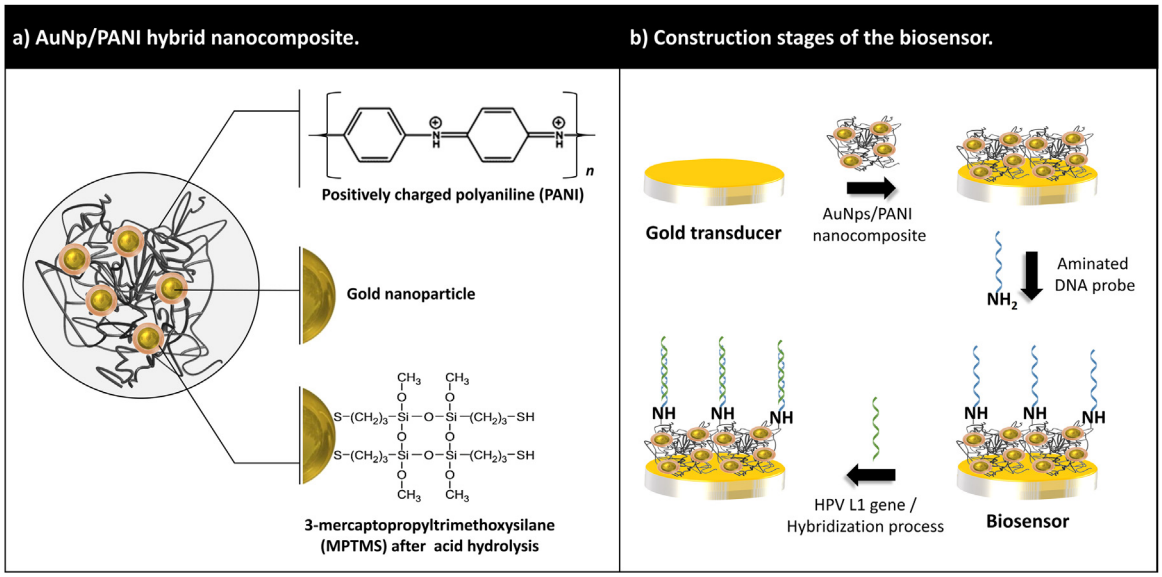

Fig. 1. Schematic representation of the AuNp/PANI hybrid nanocomposite (a) and the biosensor fabrication process (b). Glutaraldehyde is a bifunctional crosslinking agent and was used to form Shiff bases between the aminated DNA probe and the PANI amino groups.

rinsed and sonicated in deionized water for 10 min to remove residual particles. The self-assembly method was used to structure the AuNp/PANI hybrid nanocomposite on the electrode surface. This procedure was based on chemical interactions established between the thiol groups (-SH) of the nanocomposite and the gold electrode. In this step, the electrode was immersed in an ethanolic solution of AuNp/PANI with a dilution factor of 1:750 (AuNp/PANI:ethanol, v/v) for 2 min at room temperature. Subsequently, the AuNp/PANI-modified electrode was rinsed with deionized water to remove non-bonded particles.

Aminated DNA probes were immobilized on the nanostructured platform using the drop-coating method. 2 μL of glutaraldehyde (0.5 %) and 2 μL of the oligonucleotide solution (20 μM) were added to AuNp/PANI-modified electrode. Glutaraldehyde, a bifunctional crosslinking agent, was used to form Shiff bases between the aminated DNA probe and the PANI amino groups [14]. The assembly process is schematically shown in Fig. 1.

2.5. Bioactivity study

Biodetection assays were performed with cDNA obtained from patients infected with different HPV types (genotypes 6, 11, 16, 31, 33, 45, and 58). Sensitivity and specificity studies were performed using variable concentrations (1, 25, 50, 75, and 100 pg μL^{-1}) of cDNA samples containing the viral genome. Besides, cDNA samples from uninfected patients were used to evaluate selectivity. The experimental protocol was based on the exposure of the biosensor to 2 μL of each sample for 15 min. Before use, cDNA samples were heated to 94 °C for DNA denaturation.

2.6. Electrochemical measurements

Electrochemical measurements were performed using a conventional three-electrode system interfaced with a PGSTAT 128 N potentiostat/galvanostat (Metrohm Autolab Inc., Netherlands). The electrical circuit analysis was performed with the NOVA 1.11 software. The working electrode was a bare gold electrode and platinum wire and Ag/AgCl electrode saturated with KCl (3 M) were used as counter and reference electrodes, respectively. The impedance spectra were recorded in the 100 mHz and 100 kHz frequency range with an alternating voltage adjusted to an amplitude of 10 mV.

The CV analysis was performed in the -0.2 V and +0.7 V potential range at a scan rate of 50 mV s^{-1}. The electrolytic solution was 10 mM $K_4[Fe(CN)_6]^{4-}/K_3[Fe(CN)_6]^{3-}$ (1:1, v/v) in 20 mM PBS (pH 7.4). All electrochemical measurements were performed in triplicate (n = 3) using three independent electrodes to evaluate the reproducibility. The electrochemical experiments were performed at room temperature inside a Faraday cage.

2.7. Atomic force microscopy measurements

Topographic measurements were performed using an SPM-9500 atomic force microscope (Shimadzu, Japan). AFM images were acquired through an aluminum-coated silicon cantilever with a resonance frequency of 75 kHz and a force constant of 3 N m^{-1} (Multi 75AL, NCHR) in a non-contact mode. The lateral resolution was set to 512 × 512 pixels in a scan area of 5 × 5 μm. Also, the images were processed and analyzed using Gwyddion software.

3. Results and discussion

3.1. Topographic analyses

Two and three-dimensional AFM images of the electrode surface modifications are shown in Fig. 2. A well-distributed AuNp/PANI self-assembled monolayer was chemisorbed on the electrode surface (Fig. 2a). The immobilization process occurs as a result of the chemical interaction between the gold electrode surface and the terminal thiol groups (-SH) from MPTMS. The average roughness of the AuNp/PANI nanocomposite film was 8 nm. According to Dey et al. [15], AuNps are uniformly distributed on the PANI matrix due to the electrostatic interactions between positively-charged PANI and negatively-charged AuNPs. After immobilization of the recognition probe, a maximum height of 13 nm was observed (Fig. 2b). The difference of 5 nm between the heights of the AuNp/PANI and AuNp/PANI-$Probe_{HPV}$ films corresponds to the approximate size of DNA sequences composed of 20 nucleotides [16].

In Figs. 2c-d, we present the topography of the biosensor after its exposure to clinical samples from patients infected with HPV11 and 16, respectively. A noticeable increase in the height and roughness

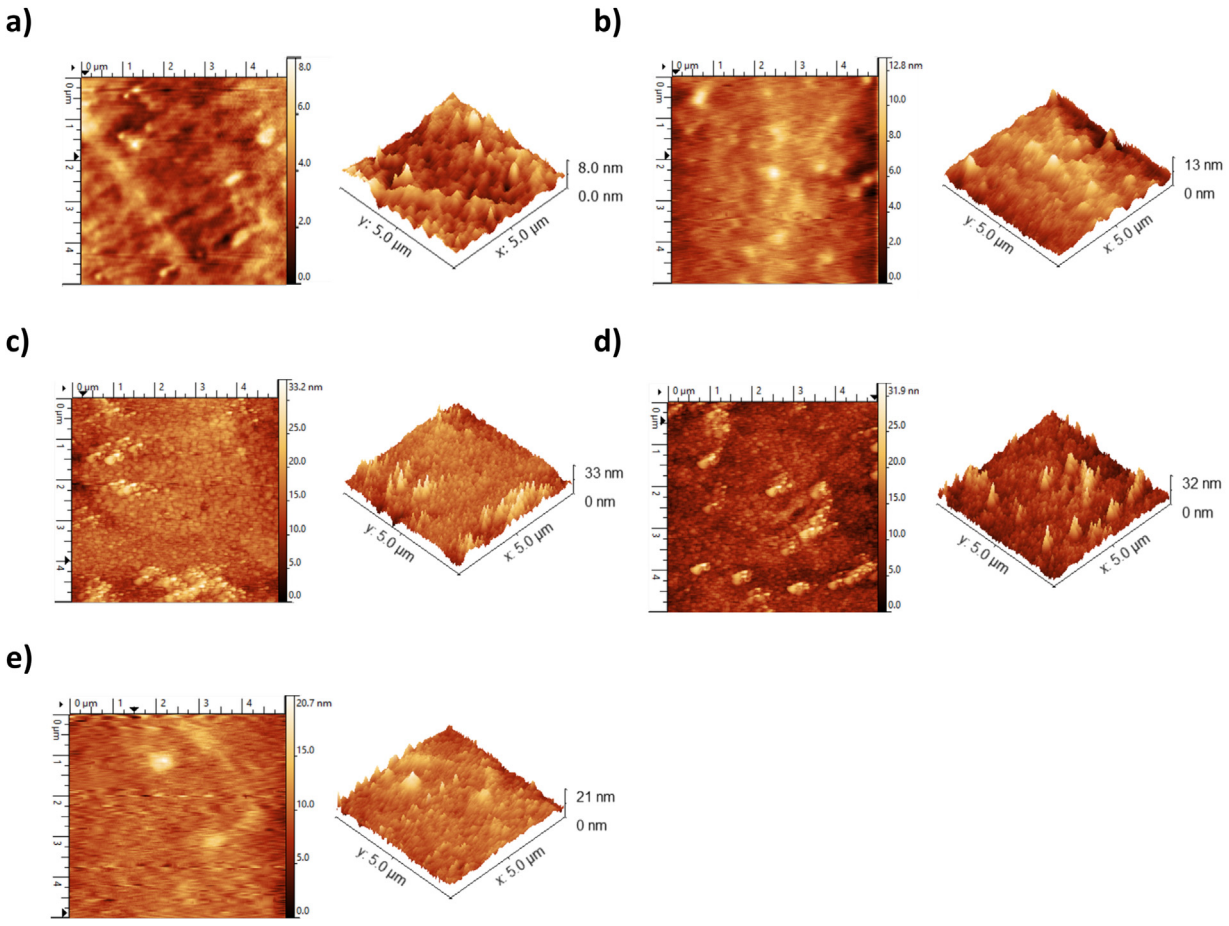

Fig. 2. AFM topographic images of the AuNp/PANI nanocomposite (a), AuNp/PANI-Probe$_{HPV}$ (b), AuNp/PANI-Probe$_{HPV}$-HPV11 (c), AuNp/PANI-Probe$_{HPV}$-HPV16 (d), AuNp/PANI-Probe$_{HPV}$-uninfected sample, with the corresponding cross-section. Scan area of 5 µm × 5 µm.

of the sensor system was observed. The presence of peaks with 33 nm (Fig. 2c) and 32 nm (Fig. 2d) heights demonstrate the ability of the biodevice to detect different HPV genotypes. The biosensor interaction with a clinical sample from uninfected patients does not cause significant morphological alterations (Fig. 2e). The difference of height between the AuNp/PANI-Probe$_{HPV}$ and AuNp/PANI-Probe$_{HPV}$-uninfected sample films can be attributed to non-specific adsorption on the sensor surface [8]. Morphological characterization of the AuNp/PANI nanocomposite using transmission electron microscopy (TEM) and scanning electron microscopy (SEM) can be seen in our previous works [17,18].

3.2. Electrochemical characterization

Fig. 3 shows the electrochemical responses of the bare gold electrode, AuNp/PANI-modified electrode, and AuNp/PANI-Probe$_{HPV}$-modified electrode. The gold electrode presents well-defined anodic/cathodic peaks with a reversible charge transfer rate in the presence of $Fe(CN)_6^{3-}/Fe(CN)_6^{4-}$ solution (Fig. 3a). The voltammetric response is decreased (33.28 to 21.94 µA) after adding AuNp/PANI nanocomposite on the electrode surface. The partial blockage of the oxidation-reduction process is related to the formation of a hybrid composite monolayer on the electroactive area.

Subsequently, a DNA probe for the detection of different HPV genotypes was chemically immobilized on the AuNp/PANI-modified electrode. The immobilization process was based on chemical bonds between terminal amine groups of the functionalized DNA probe (5′-NH_2) and PANI. The conjugation reaction was performed using glutaraldehyde as a bifunctional cross-linking agent [14]. A reduction in the anodic current signal (21.94 to 15.09 µA) was observed after the electrode modification with the biorecognition probe. This behavior is due to electrostatic repulsion between the negatively charged DNA phosphates and the negative redox probe.

Impedance spectra were recorded in the 100 mHz to 100 kHz frequency range. A modified Randles equivalent circuit (inset of Fig. 3b) was used for the theoretical simulation through the NOVA 1.11 software. The circuit includes (i) the solution (ohmic) resistance, R_S, (ii) the Warburg impedance Z_W, (iii) the constant phase element CPE, and (iv) the charge transfer resistance R_{CT}. R_S and Z_W are related to the bulk properties of the redox solution and diffusion of the electroactive species, which are not affected by biochemical reactions that occur in the electrode surface, while R_{CT} and CPE are associated with the dielectric characteristics of the electrode/electrolyte interface. The diameter of the Cole-Cole semicircle is related to the value of the R_{CT} related to electron transfer kinetics of the redox probe at the electrode interface. The values of the equivalent circuit elements obtained from the fitting of the impedance results are shown in Table S1.

The bare gold electrode spectrum is characterized by a small semi-circle at a high-frequency domain and a low R_{CT} value (R_{CT} = 0.24 kΩ) (Fig. 3b). An increase in the impedimetric response (R_{CT} = 2.64 kΩ) was observed after the modification of the electrode surface with AuNp/PANI nanocomposite. The magnitude of the impedimetric response for AuNp/PANI-Probe$_{HPV}$ electrode increased (R_{CT} = 5.04 kΩ), revealing a hindrance in the charge transfer due to the insulating behavior of the DNA probe. The immobilization of oligonucleotide sequences can cause conformational

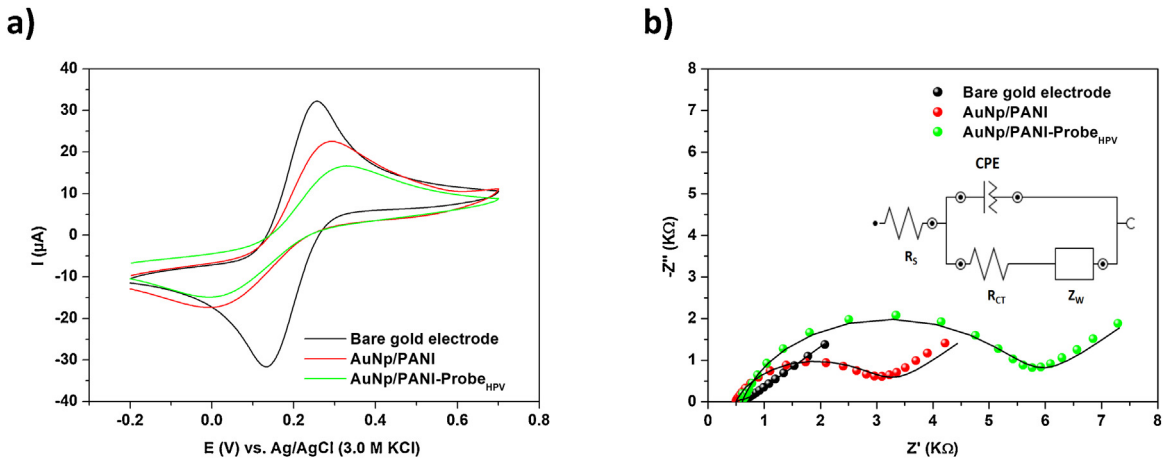

Fig. 3. Cyclic voltammograms (a) and impedance spectra (b) for each step of assembly of the biosensor. Inset: Randle's equivalent circuit used to fit the impedance measurements.

changes associated with the variation in the conductivity of the PANI, which contributes to the increase of interfacial resistance. In our previous studies [13,19,20], FT-IR spectra show PANI characteristic peaks at 1303 cm^{-1} (CN— stretching band), 1566 cm^{-1} (CC= stretching of the quinoid ring) and 1479 cm^{-1} (CC= stretching of the benzenoid ring). Evidence of the interaction between PANI and DNA is associated with the peaks at 1599 cm^{-1} (CO= stretching of cytosine/thymine nitrogenous bases and in-plane vibration of thymine) and 1642 cm^{-1} (CO= stretch of guanine/thymine and NH— stretching of thymine).

A substantial amount of research has been conducted in the biomedical field using nanocomposite materials. In 2013, Santos et al. [13] reported a simple method to prepare colloidal particles of AuNp/PANI with noticeable fluorescence in the blue and green regions of the visible spectrum. This optical characteristic revealed the potential use of the nanocomposite as a fluorescent marker for the identification of biological molecules. In addition, AuNp/PANI hybrid composite has been incorporated into nanostructured platforms for the obtaining of electrochemical biosensors with high analytical performance, selectivity and sensitivity. Recently, AuNp/PANI hybrid composite was employed for the molecular diagnosis of cancer, specifically, chronic myelogenous leukemia and acute lymphocytic leukemia, through the identification of the BCR/ABL fusion gene with a LOD in order of attomolar [8]. Furthermore, transducers modified with AuNp/PANI hybrid composite were used for label-free biodetection of dengue virus serotypes and viral glycoproteins [17], with recognition time of 10–15 min. Given these applications, the bioactivity of the proposed device in this paper will be presented below, aiming at the detection and identification of different HPV genotypes.

3.3. Sensitivity and selectivity assays

The sensitivity of the biosensor was evaluated through its exposure to different concentrations of cDNA samples from patients infected with HPV11 and HPV16 (1, 25, 50, 75, and 100 pg μL^{-1}). A reduction in the voltammetric responses associated with a decrease in the oxidation/reduction currents was observed after the biorecognition process (Fig. 4a-b). These results confirm the formation of a hybrid DNA-complex between the probe and the HPV11/HPV16 L1 gene. The decrease in the voltammetric response corresponds to an insulating effect caused by the structure of the double helix on the biosensor surface.

The bioactivity of the sensor system against samples containing the HPV11 and HPV16 genotypes can be represented by the percentage of the relative deviation of the anodic current variation (ΔI) [8].

$$\Delta I\,(\%) = \frac{I_b - I_a}{I_b} \times 100 \quad (1)$$

Where I_b and I_a correspond to the anodic peak current before and after the hybridization process, respectively. The voltammetric anodic shift for the biosensor after its interaction with different concentrations of the clinical samples is shown in Table S2. An increase in the magnitude of the ΔI was observed due to the increase of the concentrations of the analyzed samples.

The selectivity was evaluated using cDNA sample from a non-HPV infected patient at a concentration of 100 pg μL^{-1}. An insignificant change in ΔI ($\Delta I = 7.75\,\%$) was observed after the interaction of the biosensor with the test sample. ΔI for the biosensor exposed to the HPV-negative sample ($\Delta I = 7.75\,\%$) was significantly lower than the ΔI obtained during assays with HPV positive clinical specimens at the same concentration (ΔI_{HPV11} = 69.98 % and ΔI_{HPV16} = 79.32 %) (Table S2). These results indicate that HPV-negative samples may produce a low variation in the voltammetric response. The discrete decrease in the oxidation current is probably due to the physical adsorption of non-complementary DNA sequences [8]. The selectivity of the biosensor to HPV is associated with the higher electrochemical response.

In Fig. 4c-d we show the Nyquist diagrams after the biosensor was exposed to cDNA samples from patients infected with HPV11 and HPV16. The interaction of the biosensor with the patient samples results in increasing the diameter of the Cole-Cole semicircles. The relative variation of the R_{CT} (ΔR_{CT}) was used to characterize the analytical performance of the impedimetric biosensor, as follows [16].

$$\Delta R_{CT}\,(\%) = \frac{R_{CT(Biosensor-HPV)} - R_{CT(Biosensor)}}{R_{CT(Biosensor)}} \times 100, \quad (2)$$

Where $R_{CT(Biosensor\text{-}HPV)}$ is the measured value after recognition of the target DNA, and $R_{CT(Biosensor)}$ corresponds to the initial response of the biosensor (AuNp/PANI-$Probe_{HPV}$) (Table S1). Of note, ΔR_{CT} is commonly employed to calculate calibration plots of electrochemical biosensors. ΔR_{CT} values (%) are accurate to evaluate the biorecognition process [21].

A linear sensitivity response ranging from 1 to 100 pg μL^{-1} was obtained for the biosensor. The linear regression equations were expressed as $y = 61.32062 + 1.77607^{*}x$ for HPV11 (R^2 = 0.9988) and $y = 100.32791 + 2.07034^{*}x$ for HPV16 (R^2 = 0.9947) (inset of Fig. 4c-d). The y values correspond to ΔR_{CT} and the x values to the concentration (pg μL^{-1}) of the cDNA sample from a patient infected with HPV.

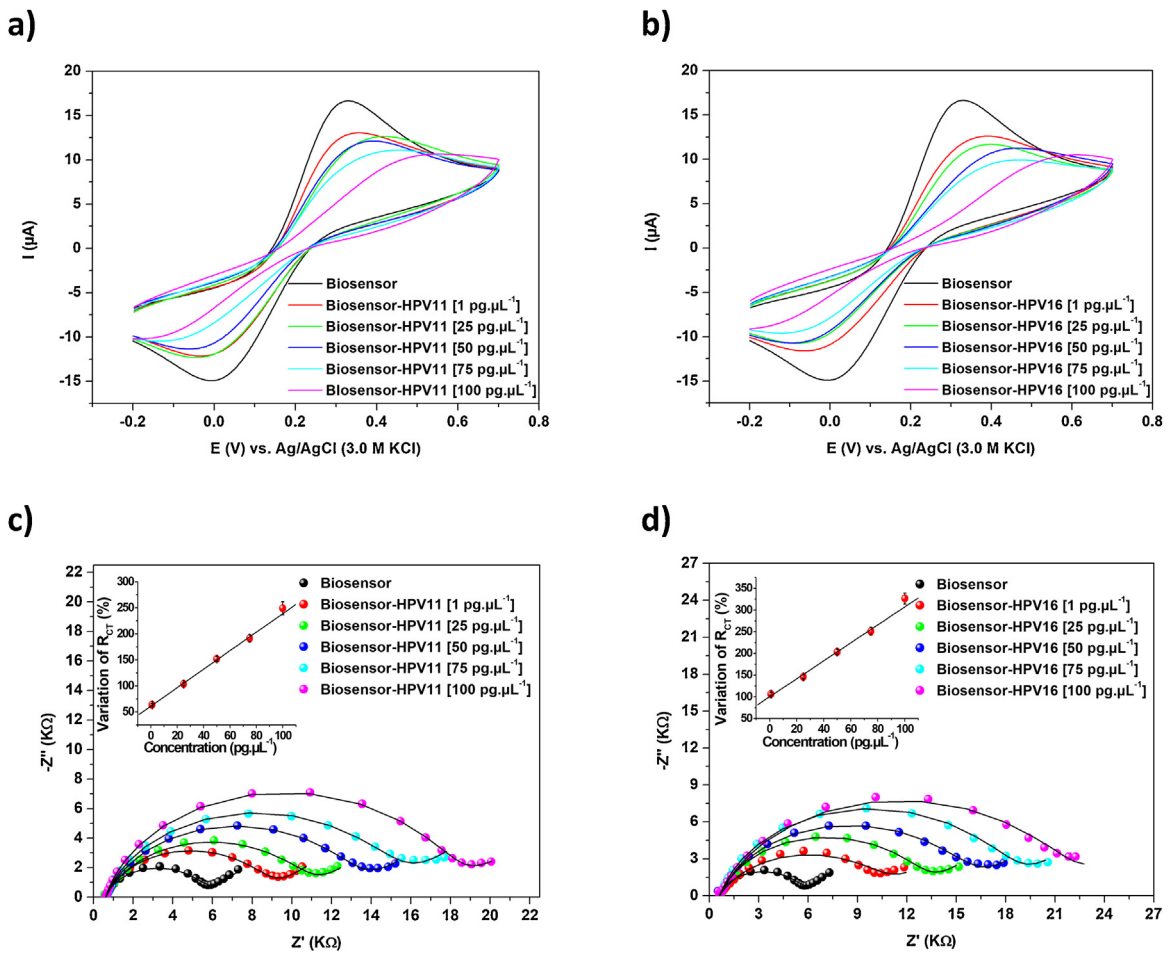

Fig. 4. Cyclic voltammograms (a and b) and impedance spectra (c and d) obtained after exposure of the biosensor to clinical samples from patients infected with HPV11 and HPV16 in variable concentrations (1, 25, 50, 75, and 100 pg μL^{-1}). Inset: Calibration plot of the biosensor for HPV11 (c) and HPV16 (d). Three replicates for each experimental condition were used. Experimental values are described as the mean values ± their half-deviation.

The LOD of the biosensor was estimated as 2.74 pg μL^{-1} and 7.43 pg μL^{-1} for HPV11 and HPV16, respectively. The LOD may be expressed as 3.3σ/slope, where σ is the standard deviation of blank measurement and the slope corresponds to the angular coefficient of the linear regression equation [22]. We emphasize that reproducibility was expressed as a percentage value of the standard deviation for three individual biosensors obtained under the same experimental conditions. The relative standard deviation was equivalent to 7.74 % (Table S1). This value indicated that the reproducibility of the biosensors was feasible. The repeatability was confirmed by a relative standard deviation of 4.43 % and 6.09 % for HPV11 and HPV16, respectively. The analysis was performed for three times in a single day, using samples with a concentration of 100 pg μL^{-1}.

The selectivity was also evaluated in terms of ΔR_{CT}, where a value of 14.09 % was obtained after the exposition of the biosensor to cDNA sample from non-HPV infected patients. The interaction of the biosensor with non-complementary DNA results in low impedimetric response due to non-specific recognition. Compared to ΔR_{CT} obtained during tests with HPV positive clinical specimens at the same concentration ($\Delta R_{CT(HPV11)}$ = 249.21 % and $\Delta R_{CT(HPV16)}$ = 326.59 %), the variation of 14.09 % is very small. This fact reflects the selectivity of the analytical system for HPV detection.

3.4. HPV identification in cervical specimens

Recognition probe design is a crucial step for the success of the genomic screening. As described in the literature, MY11 degenerate probe has been extensively used in conventional diagnostic techniques, such as RT-PCR or qRT-PCR, to demonstrate the positivity for HPV [23]. Of note, MY11 probe can detect all HPV genotypes in biological samples; however, it is not capable of distinguishing them. In this work, MY11 probe was used to identify the HPV L1 gene in electrochemical biosensing assays.

Also, tests were performed with HPV6, HPV31, HPV33, HPV45, and HPV58 to verify the specificity of the DNA biosensor with other HPV genotypes. Quantification of the apparent electrode coverage (θ) after exposure of the DNA biosensor to clinical samples can be calculated by the following equation [16]:

$$\theta = 1 - \frac{R_{CT(Biosensor)}}{R_{CT(Biosensor-HPV)}} \quad (3)$$

where $R_{CT(Biosensor)}$ is the R_{CT} value of the biosensor (AuNp/PANI-ProbeHPV) and $R_{CT(Biosensor-HPV)}$ is the corresponding value for the biosensor after exposure to clinical samples. The surface coverage is related to the number of HPV L1 gene sequences hybridized with a DNA probe on the sensor surface. The bioactivity of the sensor with different HPV genotypes and θ values were presented in Fig. S1. The degree of electrode coverage ranged from 63.50 ± 1.85 % to 80.31 ± 1.15 % for clinical samples from patients infected with HPV. These results can be correlated with the detection capacity of the biosensor for HPV types. θ value of 12.21 ± 4.28 % was obtained for the uninfected sample. Thus, this result demonstrates low non-specific adsorption of oligonucleotide sequences, indicating the specificity of the biosensor for HPV genotypes.

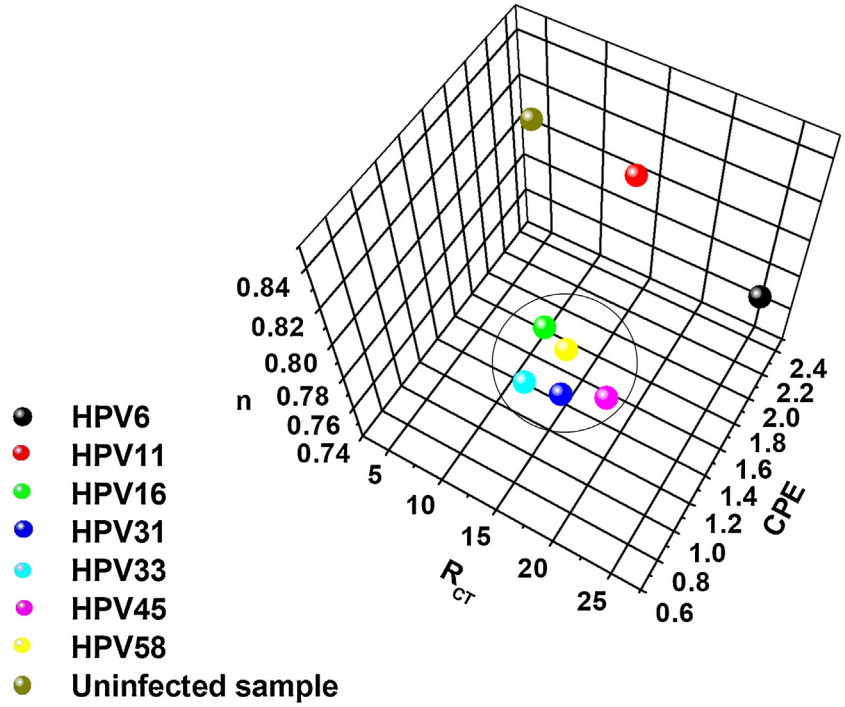

Fig. 5. Three-dimensional plot for the R_{CT}, CPE, and n variables obtained from the theoretical simulation of the Nyquist spectra.

Table 1
Analytical comparison between the proposed biosensor and other genosensors reported in the literature for HPV detection.

Biosensitive system	DNA target	Analytical technique	Detection strategy	Detection time	Detection range	Limit of detection	Reference
Gold surface – AuNp/PANI – probe	HPV11HPV16	CV and EIS	Label-free electrochemical	15 min	1 pg/μL to 100 pg/μL	2.74 pg/μL 7.43 pg/μL	This work
Pencil graphite surface – HPV 16 E6 probe	HPV16	DPV	Label-free electrochemical	5 min	5 pg/μL to 40 pg/μL	16 pg/μL	[26]
Pencil graphite surface – probe	HPV (L1 gene)	SWV	Labeled electrochemical (methylene blue)	3 min	1.2 ng/μL to 50 ng/μL	1.2 ng/μL	[27]
IDE chip – ZnO Nanorods – AuNP – probe	HPV16	EIS	Label-free electrochemical	10 min	10^{-7} M to 10^{-15} M	1 fM	[30]
Copper oxide nanoparticles functionalized with streptavidin – biotinylated capture probe	HPV16	SERS	Optical	10 min	5 nM to 100 nM	1 nM	[28]
Magnetic glass particles – probe	HPV	Fluorescence spectrophotometry	Optical (CdTe/ZnSe core/shell quantum dots used as fluorescence label)	90 min	–	0.0125 ng/μL	[29]

DPV – Differential pulse voltammetry.
SWV – Square wave voltammetry.
SERS – Surface-enhanced Raman scattering.

The interpolation of the R_{CT}, CPE and n variables obtained from the theoretical simulation of the Nyquist spectra enabled the construction of a 3D plot (Fig. 5). The sensor showed distinct electrochemical responses for HPV genotypes of high (HPV16, HPV31, HPV33, HPV45, and HPV58) and low oncogenic risk (HPV6 and HPV11). The recognition profiles were associated with phylogenetic characteristics of the papillomavirus. Of note, HPV genotypes of high and low oncogenic risk are related to different phylogenetic branches [24]. Conserved regions of the viral genome (e.g., L1 gene) can undergo substitution of nucleotide bases in the same viral family.

Degenerate DNA probes provide only positive or negative responses to the presence of HPV in clinical specimens [25] and can be used for the simultaneous detection of different viral strains. To the best of our knowledge, this is the first time that an electrochemical biosensor for HPV genotypes is capable of differentiating high and low oncogenic risk using a degenerate DNA probe. HPV genotypes are characterized by subtle genome dissimilarities and, therefore, different electrochemical responses can be obtained.

3.5. Comparative study

Table 1 shows an analytical comparison between the proposed biosensor and the other DNA biosensors reported in the literature for HPV detection. PCR and hybrid capture assays are the main molecular techniques for HPV research in clinical labora-

tories. However, these methodologies present disadvantages as false-positive results due to contamination with previously amplified material, time-consuming procedures, and limited sensitivity. In particular, we can highlight the Hybrid Capture® 2 assay (QIAGEN, Gaithersburg, MD, USA) based on the use of two DNA probes to distinguish between high-risk and low-risk HPV groups [3].

Currently, a wide variety of optical and electrochemical biosensors has been developed for the detection of HPV genotypes [26–29]. However, genotype discrimination is possible with the use of specific oligonucleotides for each papillomavirus [23]. The present report demonstrates that the degenerate MY11 probe is useful for the detection and identification of HPV genotypes through electrochemical techniques.

4. Conclusions

In this paper, we used a degenerate DNA probe for the development of a label-free biosensor, allowing the detection and genotyping of HPV strains in clinical specimens.

A degenerate oligonucleotide sequence was successfully immobilized on the AuNp/PANI nanocomposite. The proposed biosensor is the only described in the literature that suggests an electrochemical differentiation of high and low-risk genotypes through a degenerate DNA probe. This differentiation between HPV strains is relevant to assess potentially oncogenic infections and prevent the development of cervical cancer. Commonly, degenerate probes are applied in convencional molecular methods to analyze the virus presence, without identifying the particular strain. The association between PANI and AuNPs provides an innovative hybrid material with improved physicochemical properties, large surface area, biological compatibility and easy biofunctionalization. A new DNA biosensor was obtained with wide detection range (1 pg μL^{-1} to 100 pg μL^{-1}), high sensitivity (LOD_{HPV11} = 2.74 pg μL^{-1}; LOD_{HPV16} = 7.43 pg μL^{-1}), selectivity, and specificity. The obtained nanosensor can be considered a valid alternative for HPV diagnosis in the clinical specimens with distinction of phylogenetic characteristics.

Declaration of Competing Interest

The authors declare that there are no competing interests for publication of this paper. Statement

Acknowledgments

This work was supported by the Brazilian National Council for Scientific and Technological Development/CNPq [grant numbers 302885/2015-3, 310364/2015-9, 302930/2015-9, 314894/2018-7 and 314756/2018-3]; the Brazilian Health Ministry Project DECIT-FINEP-CNPq [grant numbers 1299/2013 and 401700/2015-1]; and the FACEPE-PPSUS-APQ [grant number 0040-4.00/13]. Avelino would like to thank CAPES for a pH.D. scholarship.

Appendix A. Supplementary data

Supplementary material related to this article can be found, in the online version, at doi:https://doi.org/10.1016/j.jpba.2020.113249.

References

[1] B. Serrano, M. Brotons, F.X. Bosch, L. Bruni, Epidemiology and burden of HPV-related disease, Best Pract. Res. Clin. Obstet. Gynaecol. 47 (2018) 14–26.
[2] H. Huang, W. Bai, C. Dong, R. Guo, Z. Liu, An ultrasensitive electrochemical DNA biosensor based on graphene/Au nanorod/polythionine for human papillomavirus DNA detection, Biosens. Bioelectron. 68 (2015) 442–446.
[3] E. Rasouli, Z. Shahnavaz, W.J. Basirun, M. Rezayi, A. Avan, M. Ghayour-Mobarhan, et al., Advancements in electrochemical DNA sensor for detection of human papilloma virus? a review, Anal. Biochem. (2018).
[4] P. Mahmoodi, M. Fani, M. Rezayi, A. Avan, Z. Pasdar, E. Karimi, et al., Early detection of cervical cancer based on high-risk HPV DNA-based genosensors: a systematic review, BioFactors 45 (2019) 101–117, http://dx.doi.org/10.1002/biof.1465.
[5] D. Sadighbayan, K. Sadighbayan, A.Y. Khosroushahi, M. Hasanzadeh, Recent advances on the DNA-based electrochemical biosensing of cancer biomarkers: analytical approach, Trac Trends Anal. Chem. 119 (2019) 1–29, http://dx.doi.org/10.1016/j.trac.2019.07.020.
[6] E.E. Ferapontova, DNA electrochemistry and electrochemical sensors for nucleic acids, Annu. Rev. Anal. Chem. 11 (2018) 197–218.
[7] S. Shrivastava, N. Jadon, R. Jain, Next-generation polymer nanocomposite-based electrochemical sensors and biosensors: a review, Trac Trends Anal. Chem. 82 (2016) 55–67.
[8] K.Y.P.S. Avelino, I.A.M. Frias, N. Lucena-Silva, R.G. Gomes, C.P. de Melo, M.D.L. Oliveira, et al., Attomolar electrochemical detection of the BCR/ABL fusion gene based on an amplifying self-signal metal nanoparticle-conducting polymer hybrid composite, Colloids Surf. B Biointerfaces 148 (2016) 576–584.
[9] N. Elahi, M. Kamali, M.H. Baghersad, Recent biomedical applications of gold nanoparticles: a review, Talanta 184 (2018) 537–556, http://dx.doi.org/10.1016/j.talanta.2018.02.088.
[10] S. Kumar, W. Ahlawat, R. Kumar, N. Dilbaghi, Graphene, carbon nanotubes, zinc oxide and gold as elite nanomaterials for fabrication of biosensors for healthcare, Biosens. Bioelectron. 70 (2015) 498–503.
[11] F. Ran, Y. Tan, W. Dong, Z. Liu, L. Kong, L. Kang, In situ polymerization and reduction to fabricate gold nanoparticle-incorporated polyaniline as supercapacitor electrode materials, Polym. Adv. Technol. 29 (2018) 1697–1705.
[12] C. Dhand, M. Das, M. Datta, B. Malhotra, Recent advances in polyaniline based biosensors, Biosens. Bioelectron. 26 (2011) 2811–2821.
[13] R.F.S. Santos, C.A.S. Andrade, C.G. dos Santos, C.P. de Melo, Visible luminescence in polyaniline/(gold nanoparticle) composites, J. Nanoparticle Res. 15 (2013) 1408.
[14] R. Singh, C. Dhand, G. Sumana, R. Verma, S. Sood, R.K. Gupta, et al., Polyaniline/carbon nanotubes platform for sexually transmitted disease detection, J. Mol. Recognit. 23 (2010) 472–479.
[15] A. Dey, A. Kaushik, S.K. Arya, S. Bhansali, Mediator free highly sensitive polyaniline–gold hybrid nanocomposite based immunosensor for prostate-specific antigen (PSA) detection, J. Mater. Chem. 22 (2012) 14763–14772.
[16] M.P. Costa, C.A.S. Andrade, R.A. Montenegro, F.L. Melo, M.D.L. Oliveira, Self-assembled monolayers of mercaptobenzoic acid and magnetite nanoparticles as an efficient support for development of tuberculosis genosensor, J. Colloid Interface Sci. 433 (2014) 141–148.
[17] K.Y.P.S. Avelino, C.A.S. Andrade, C.P. de Melo, M.L. Nogueira, M.T.S. Correia, L.C.B.B. Coelho, et al., Biosensor based on hybrid nanocomposite and CramoLL lectin for detection of dengue glycoproteins in real samples, Synth. Met. 194 (2014) 102–108.
[18] M.F.Kd.S. Garcia, C.A.S. Andrade, C.P. de Melo, D.S. Gomes, L.G. Silva, R.V. Dias, et al., Impedimetric sensor for Leishmania infantum genome based on gold nanoparticles dispersed in polyaniline matrix, J. Chem. Technol. Biotechnol. 91 (2016) 2810–2816.
[19] G.C. Pedro, F.D. Gorza, R.J. da Silva, K.T. do Nascimento, J.C. Medina-Llamas, A.E. Chávez-Guajardo, et al., A novel nucleic acid fluorescent sensing platform based on nanostructured films of intrinsically conducting polymers, Anal. Chim. Acta 1047 (2019) 214–224.
[20] S.V. de Lima, H.P. de Oliveira, C.A. Andrade, C.P. de Melo, A dielectric study of interpolymer complexes of polyaniline and DNA, Colloids Surf. A Physicochem. Eng. Asp. 471 (2015) 139–147.
[21] A. Butterworth, E. Blues, P. Williamson, M. Cardona, L. Gray, D.K. Corrigan, SAM composition and electrode roughness affect performance of a DNA biosensor for antibiotic resistance, Biosensors 9 (2019) 22.
[22] P. Supraja, S. Tripathy, S.R.K. Vanjari, V. Singh, S.G. Singh, Electrospun tin (IV) oxide nanofiber based electrochemical sensor for ultra-sensitive and selective detection of atrazine in water at trace levels, Biosens. Bioelectron. (2019), 111441.
[23] Z. Chen, L.B. De Freitas, R.D. Burk, Evolution and classification of oncogenic human papillomavirus types and variants associated with cervical cancer, in: Cervical Cancer, Springer, 2015, pp. 3–26.
[24] M. Schiffman, R. Herrero, R. DeSalle, A. Hildesheim, S. Wacholder, A.C. Rodriguez, et al., The carcinogenicity of human papillomavirus types reflects viral evolution, Virology 337 (2005) 76–84.
[25] D. Dell'Atti, M. Zavaglia, S. Tombelli, G. Bertacca, A.O. Cavazzana, G. Bevilacqua, et al., Development of combined DNA-based piezoelectric biosensors for the simultaneous detection and genotyping of high risk Human Papilloma virus strains, Clin. Chim. Acta 383 (2007) 140–146.
[26] D.S. Campos-Ferreira, E.V. Souza, G.A. Nascimento, D.M. Zanforlin, M.S. Arruda, M.F. Beltrao, et al., Electrochemical DNA biosensor for the detection of human papillomavirus E6 gene inserted in recombinant plasmid, Arab. J. Chem. 9 (2016) 443–450.
[27] R. Sabzi, B. Sehatnia, M. Pournaghi-Azar, M. Hejazi, Electrochemical detection of human papilloma virus (HPV) target DNA using MB on pencil graphite electrode, J. Iran. Chem. Soc. 5 (2008) 476–483.

[28] Z. Yang, C. Yi, S. Lv, Y. Sheng, W. Wen, X. Zhang, et al., Development of a lateral flow strip biosensor based on copper oxide nanoparticles for rapid and sensitive detection of HPV16 DNA, Sens. Actuators B Chem. 285 (2019) 326–332.
[29] A.M.J. Jimenez, A. Moulick, S. Bhowmick, V. Strmiska, M. Gagic, Z. Horakova, et al., One-step detection of human papilloma viral infection using quantum dot-nucleotide interaction specificity, Talanta 205 (2019), 120111.
[30] T. Ramesh, K.L. Foo, R. Haarindraprasad, A.J. Sam, M. Solayappan, Gold-Hybridized Zinc oxide nanorods as Real-time Low-cost nanoBiosensors for Detection of virulent DNA signature of HPV-16 in cervical carcinoma, Sci. Rep. 9 (2019) 1–17.